# Round holes in glulam beams arranged eccentrically or in groups

Martin Danzer, Philipp Dietsch and Stefan Winter

Chair of Timber Structures and Building Construction

Technical University of Munich

Keywords: timber, glulam beams, holes, holes arranged eccentrically, groups of holes, reinforcement

## 1 Introduction

The current edition of the European Timber Design Code EN 1995-1-1 (2004) does not contain design provisions for holes in beams. The German National Annex DIN EN 1995-1-1/NA (2013) provides such design and construction rules, which are, however, restrictive with regard to the positioning of holes in the beam. Experimental investigations in the form of small- and large-scale tests and numerical investigations on round holes in glulam beams were realized considering the unreinforced as well as the reinforced state in the form of fully threaded screws and threaded rods. The objective was to generate an experimental basis for deriving a design format and to study the general structural behaviour as well as the influence of parameters like eccentricity over the beam height, clear distance between two holes and effect of reinforcement.

## 2 Experimental investigations

Basis of the experimental investigations were two test series in the form of small-scale tests ($b x h$ = 120 mm x 400 mm) and large-scale tests ($b x h$ = 200 mm x 1000 mm).

### 2.1 Test program

In Figure 1 the main configurations of the small-scale tests are shown. With respect to eccentric arrangements of individual holes the location was varied in four steps ($e/h$ = ±0.175; ±0.100), regarding groups of holes arranged in horizontal direction the

clear distance was varied in three steps ($l_z$ = 1.05$h$; 0.70$h$; 0.35$h$). To enable a comparison between the aforementioned configurations a consistent hole diameter $d/h$ = 0.35 was chosen. Groups of holes arranged in vertical direction were tested in only one configuration with a smaller hole diameter $d/h$ = 0.25 due to fewer possibilities in variation given by the geometry. The configuration for comparative tests on individual holes is not shown separately in Figure 1. For these tests, only two new specimens were available. All other configurations consisted of three specimens. The material used was glulam GL 28h. For the reinforced specimens two fully threaded screws $d$ = 10 mm arranged over the beam width were used. The inclination between screw axis and fibre direction was set to $\alpha$ = 60° in most cases, except $\alpha$ = 90° in case of the vertical group. For further information see Danzer et al. (2017).

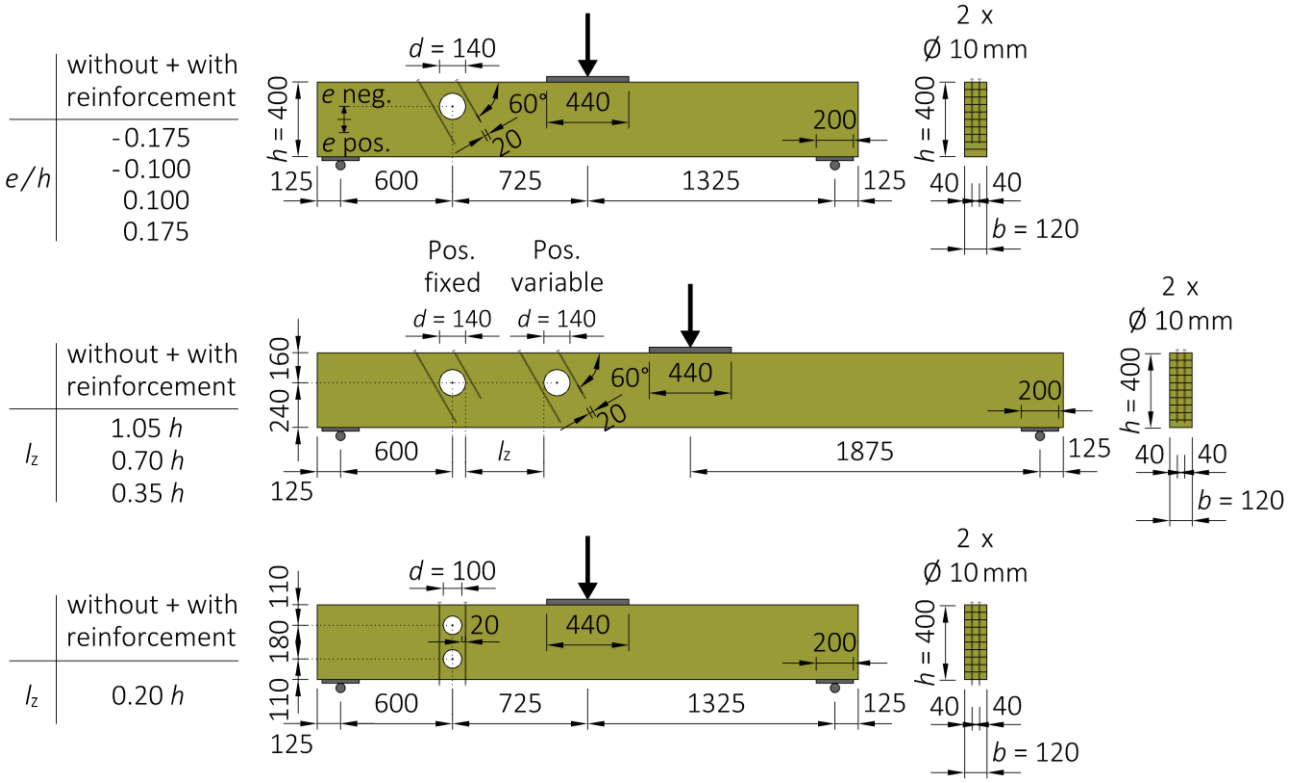


*Figure 1: Configurations of the small-scale tests*

In the large-scale tests two configurations of individual holes arranged eccentrically ($e/h$ = ±0.175), one configuration of a horizontal group ($l_z$ = 0.35$h$) and one configuration of a vertical group ($l_z$ = 0.20$h$) were tested, see Figure 2. All configurations were reinforced by two screwed-in threaded rods $d$ = 16 mm arranged over the beam width. Based on results of numerical investigations the inclination of the reinforcing elements in the configurations *individual hole (e/h = 0.175)* and *vertical group* was adapted to $\alpha$ = 45°. In addition, two configurations of individual holes ($d/h$ = 0.40; $e/h$ = ±0.100) were tested without reinforcement under pure bending moment. Each configuration consisted of four specimens. Two out of the four specimens corresponded to strength class GL 24h and two corresponded to strength class GL 28h, respectively.

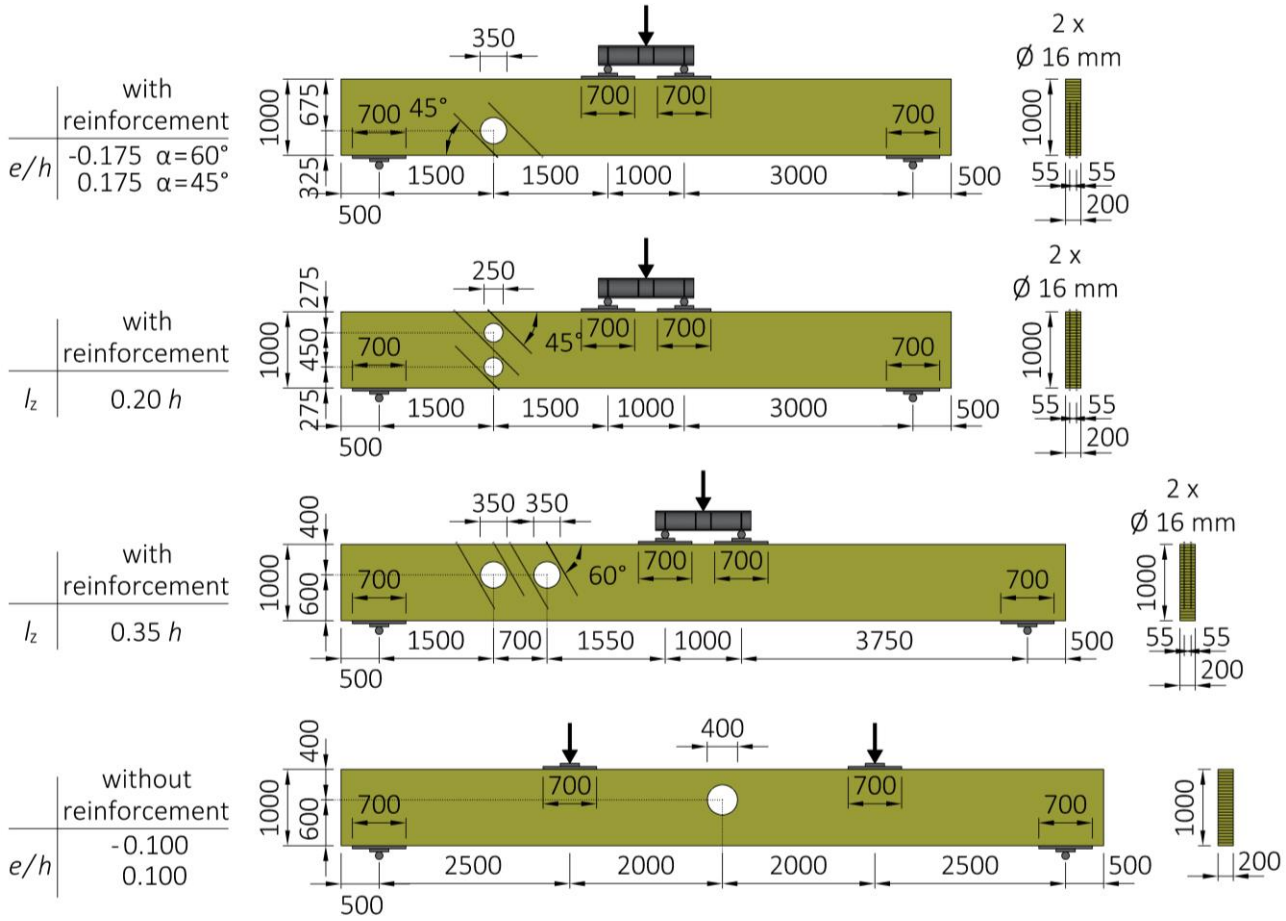


*Figure 2: Configurations of the large-scale tests*

## 2.2 Results

Due to the failure characteristics the tests results given in the following were differentiated according to the three steps *crack initiation in the middle of the cross sectional width*, *full crack over the whole beam width* and *ultimate load*.

- Individual holes arranged eccentrically ($d/h$ = 0.35)

In case of the small-scale tests in the unreinforced state only a marginal influence of the eccentricity can be stated for all three levels of failure, see Figure 3. In the reinforced state the influence of the eccentricity at the load levels *full crack* and *ultimate load* was more pronounced in the form of decreasing load-bearing capacities when grouping the eccentricity from the edge under compressive bending stresses to the edge under tensile bending stresses. In comparison to the unreinforced state load increases of up to 98% could be observed, depending on the eccentricity.

In the large-scale tests a similar structural behaviour when compared to the small-scale tests could be observed. Comparing the ratios of the ultimate loads reached for the two extreme eccentricities in both test series reveals a marginally higher value in case of the large-scale tests (0.77 instead of 0.72). This means that the adapted inclination of reinforcement ($\alpha$ = 45°) resulted in a slightly better performance.

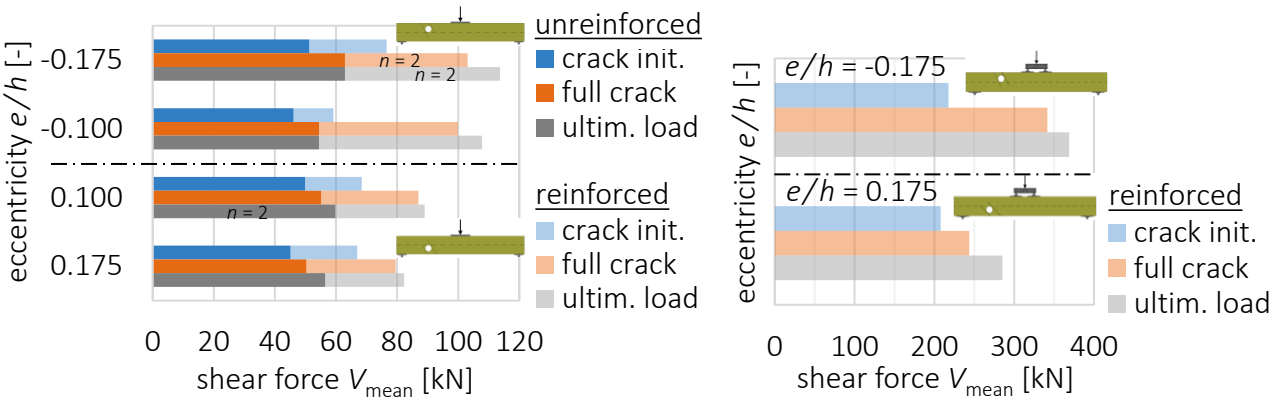


*Figure 3: Test results for individual holes arranged eccentrically (d/h = 0.35); left: small-scale tests; right: large-scale tests*

- Groups of holes arranged in horizontal direction ($d/h$ = 0.35)

In case of the small-scale tests in the unreinforced state a decreasing clear distance resulted in decreasing load-bearing capacities to a minimum level of about 73 % in case of the smallest clear distance, see Figure 4. The group arrangement with the largest clear distance failed at only negligibly lower loads when compared to the results for the individual holes. In the reinforced state neither in the small-scale tests nor in the large-scale tests a clear statement is possible at the load level *ultimate load* due to premature beam failure in global bending/shear distant to the holes.

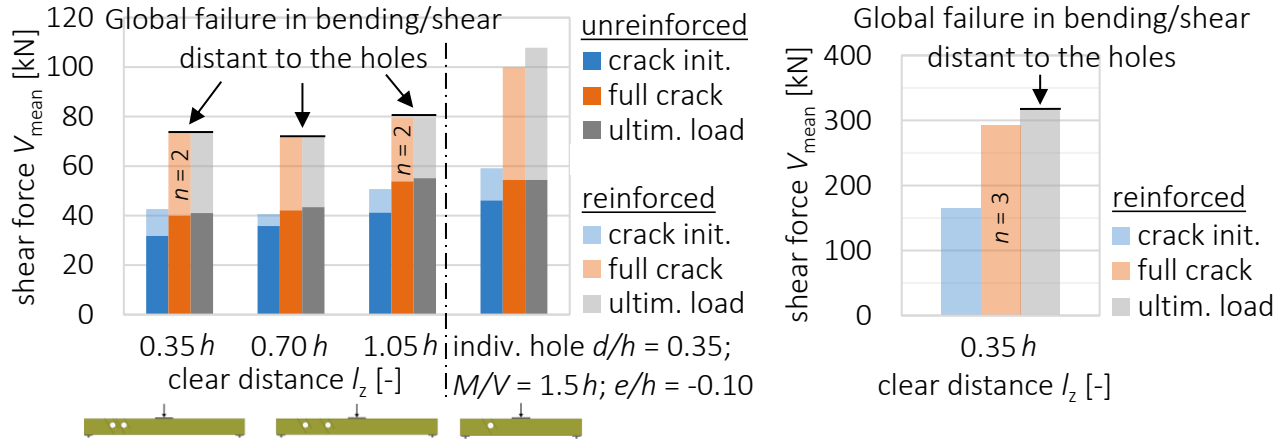


*Figure 4: Test results for groups of holes arranged in horizontal direction (d/h = 0.35); left: small-scale tests; right: large-scale tests*

- Groups of holes arranged in vertical direction ($d/h$ = 0.25)

In case of the small-scale tests in the unreinforced state only a small mutual influence of the group arrangement could be observed compared to the individual holes, see Figure 5. However, the percentage load increases in the reinforced state are small in comparison to those of the individual holes with inclined applications of the reinforcement. Reasons are different failure modes but also a small reinforcing effect as a result of an application under $\alpha$ = 90°.

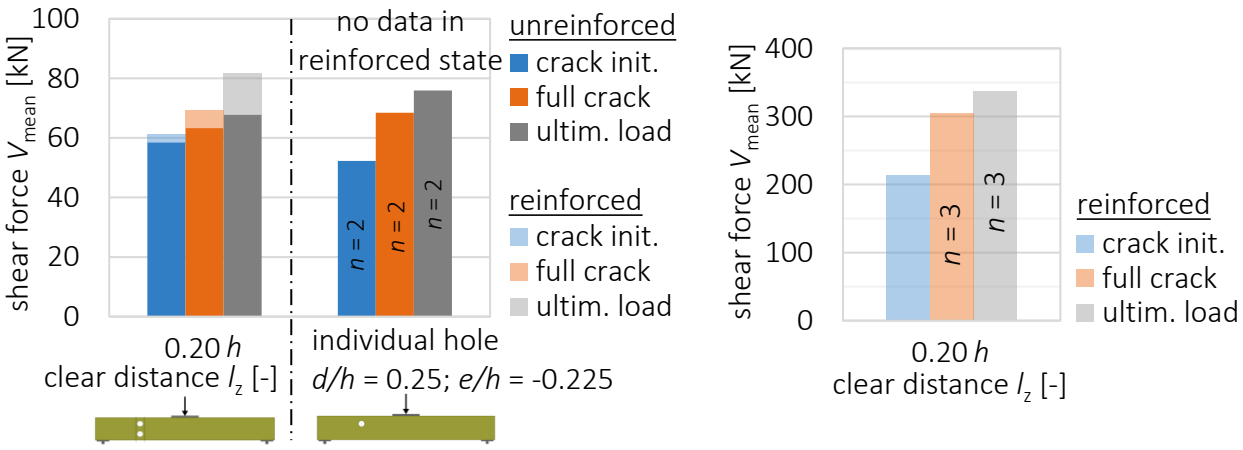


*Figure 5: Test results for groups of holes arranged in vertical direction (d/h = 0.25); left: small-scale tests; right: large-scale tests*

At ultimate load levels calculated load-bearing capacities in shear based on the gross cross-sections reveal similar values for small- and large-scale tests. The larger area exposed to shear in case of the large-scale tests, resulting in smaller estimated shear strength, indicate the higher reinforcing effect of the application under $\alpha = 45°$.

- Individual holes arranged eccentrically under pure bending moment ($d/h = 0.40$)

The observed failure of both configurations at the ultimate load level was a bending tension failure in the region of the hole. At the levels of crack initiation and full crack almost no difference in load level can be seen for the two configurations, see Figure 6. At the ultimate load level the influence of the hole located in the bending tension zone was more pronounced.

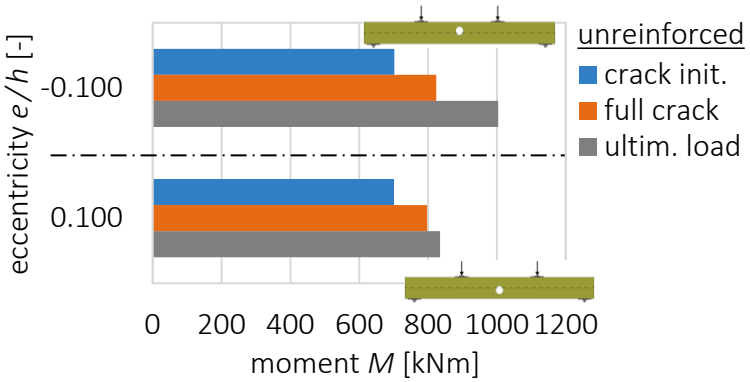


*Figure 6: Test results for individual holes arranged eccentrically under pure bending moment (d/h = 0.40)*

In addition to stresses in tension perpendicular to the grain and shear also concentrated stresses in grain direction occur close to the hole edges above and below the hole. According to numerical simulations the magnitude of these stress concentrations can be several times higher than the bending stresses at the beam edge, see Figure 7 for an exemplary location of the hole in the area of compressive bending stresses. To further investigate that behaviour strain gauges were placed on some specimens at

the hole edge inside the hole and in the direct vicinity of the hole edge as well as the beam edge.

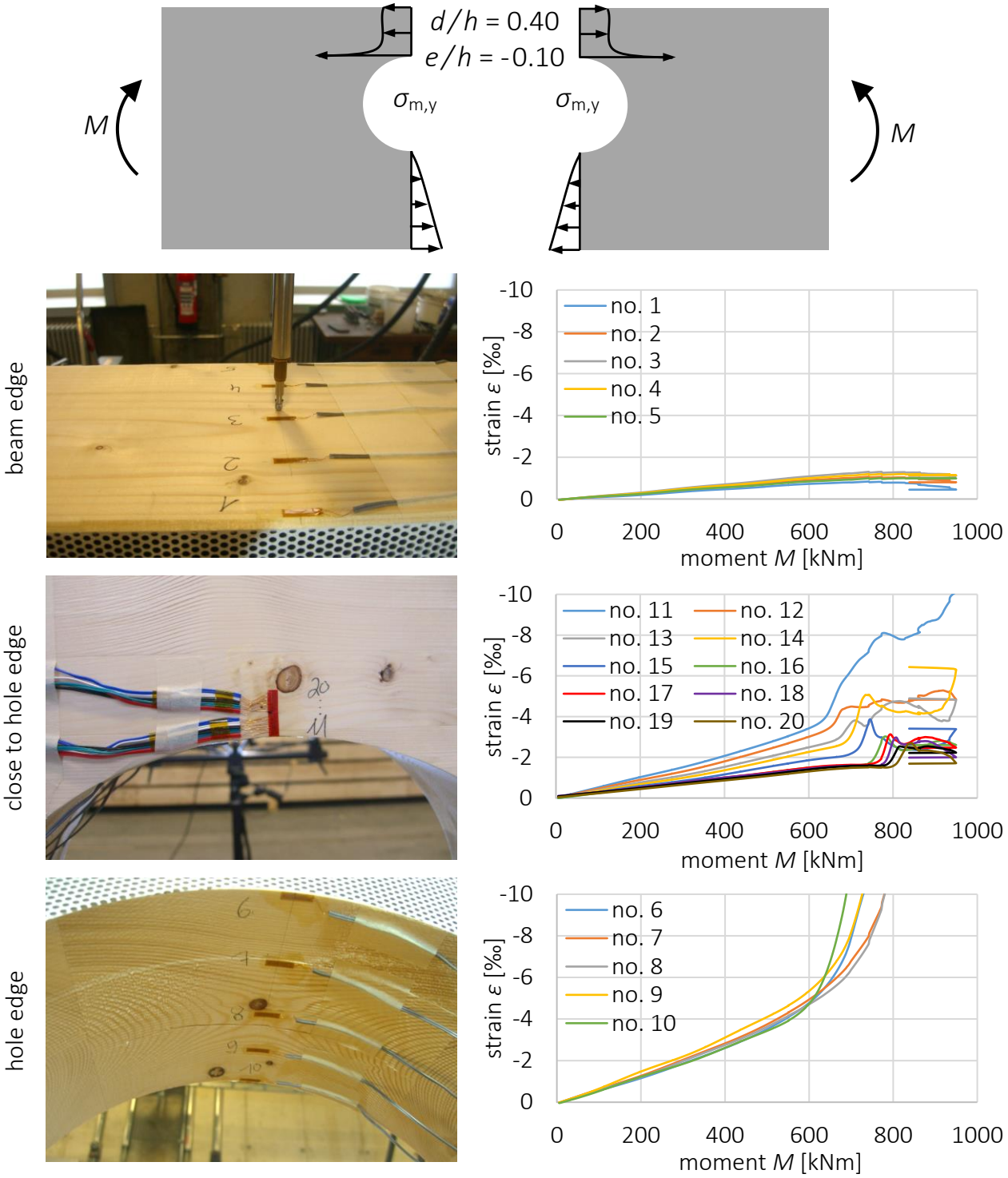


*Figure 7: Strain measurements to investigate the concentration of stresses in direction of the grain around the hole (specimen no. 1, GL 28h, e/h = -0.10)*

A comparison of the results at the hole edge and the beam edge confirms the results of the numerical investigations in the form of significantly higher values at the hole edge. Up to a moment $M$ = 600 kNm an approximately linear elastic behaviour can be observed at the hole edge. Further load increase results in a disproportionate strain increase, i.e. a plastic behaviour. Analysing the strain gauges at the side face it can be

seen that the stress concentration decreases rapidly with increasing distance to the hole edge and that the extension of the plastic zone increases with further load increase.

For the configuration with the hole in the area under bending tension also significantly higher strains were measured at the hole edge. In contrast to the arrangement in the area of compressive bending stresses a linear elastic behaviour was observed until failure at ultimate load.

# 3 Numerical investigations

## 3.1 Influence of eccentricity

In general, placing a hole in a timber beam has an effect on all three stress components, $\sigma_m$, $\sigma_{90}$ and $\tau$. The structural behaviour can always be derived from the shares of the stress distributions $\sigma_m$ and $\tau$ of the gross cross-section, which cannot be transferred through the hole and thus have to be redistributed around the hole, see Figure 8.

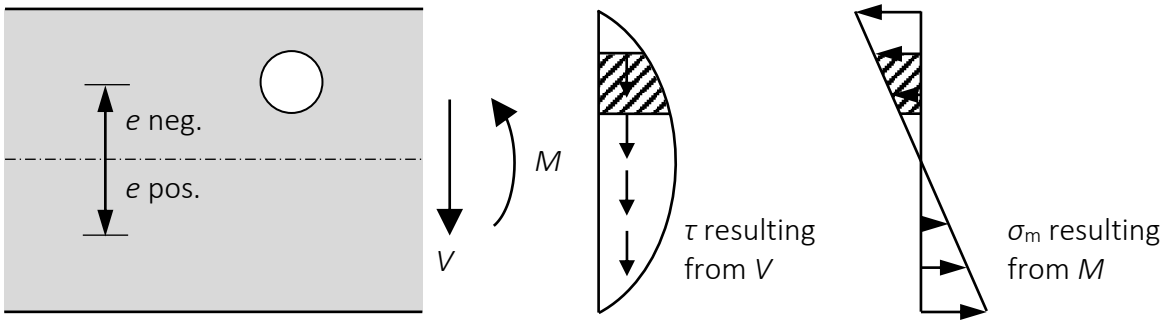


*Figure 8: Shares of the stress distributions which have to be redistributed around the hole*

In case of the distribution of shear stresses $\tau$ the magnitude of this share slightly decreases with increasing eccentricity. In case of the distribution of bending stresses $\sigma_m$ the magnitude of this share significantly increases. Thus an increasing eccentricity has a positive effect on the structural behaviour in case of a shear force $V$ and a negative effect in case of a moment $M$. For each consideration of the influence of a hole a superposition of these contrary effects of different magnitude is necessary. Thus, the location of the hole in the beam ($e/h$, $M/V$) is decisive to determine its entire effect.

Exemplarily this behaviour can be illustrated by means of resulting load-bearing capacities in tension perpendicular to the grain in the unreinforced state. Load-bearing capacities were determined by numerical simulations, that were combined to a Weibull based design approach, investigated by Höfflin (2005) for centrically located holes. In Figure 9 the resulting load-bearing capacities are shown for two different hole diameters in dependence of the location in the beam ($b \times h$ = 120 mm x 400 mm). The assumed strength in tension perpendicular to the grain for a reference volume $V_0$ = 0.01 m³ was $f_{t,90,mean}$ = 0.83 N/mm². For very small ratios of $M/V$ (marginal influence of $M$) the influence of the eccentricity is slightly positive but becomes more negative with increasing ratio $M/V$ (increasing influence of $M$).

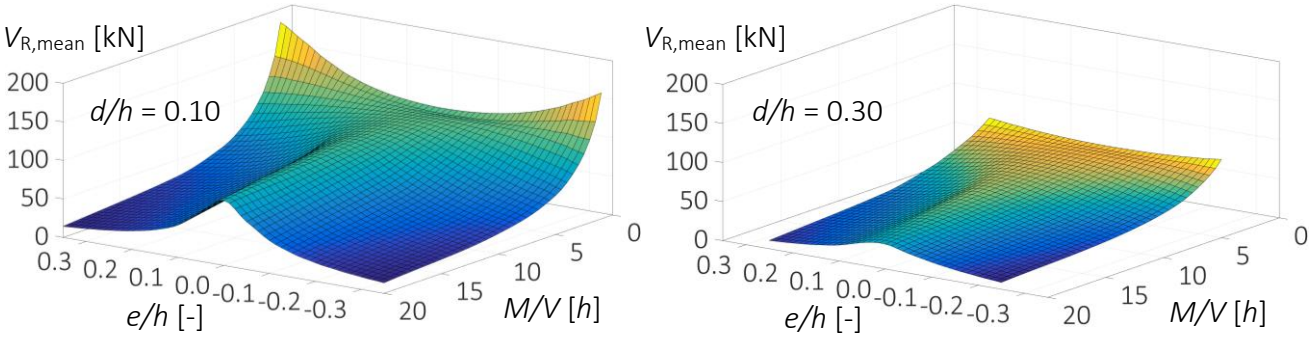


*Figure 9: Load-bearing capacities in tension perpendicular to the grain (b x h = 120 mm x 400 mm)*

## 3.2 Effect of reinforcement

To quantifiy the effect of the reinforcement, the configurations of the eccentrically located holes of the small-scale tests were investigated in numerical simulations, separating between tension perpendicular to the grain and shear. Reinforcement by two fully threaded screws $d$ = 10 mm over the beam width with different inclinations but constant distance between screw axis and hole edge was considered. For general modelling of the reinforced state, experiments to determine the axial stiffness between screw and timber and validation of the numerical model it is referred to Danzer et al. (2016) and Danzer et al. (2017).

- Effect of reinforcement regarding tension perpendicular to the grain

In Figure 10 the effect of different inclinations of the reinforcing elements regarding tension perpendicular to the grain is displayed. In analogy to the unreinforced state the Weibull-based design approach also was used for the reinforced state. Clearly visible are the higher load-bearing capacities in the cases of an inclined application. For locations of the holes in the area under compressive bending stresses $\alpha$ = 60° reveals the highest values, for locations of the holes in the area under tensile bending stresses $\alpha$ = 45° reveals the highest values.

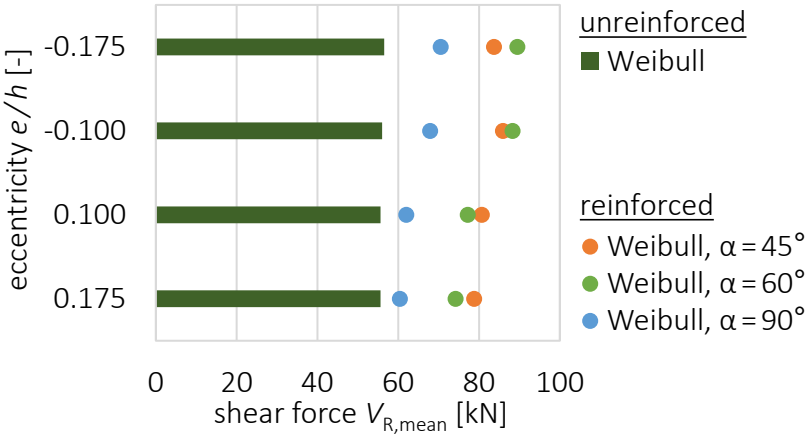


*Figure 10: Load-bearing capacities in tension perpendicular to the grain without/with reinforcement*

The numerical results determined for the unreinforced state show good agreement with the experimental results, the results determined for the reinforced state tend to

underestimate the experimental results, see Danzer et al. (2016) and Danzer et al. (2017) for an in-depth comparison.

- Effect of reinforcement regarding shear

To quantify the effect regarding shear, distributions of shear stresses were determined along two paths representing planes of potential crack formation, extended from the middle of the hole towards the beam end/midspan. In addition, the axial forces in the reinforcing elements were determined and displayed at the side of the diagrams. Figure 11 exemplarily shows the results for the eccentricity $e/h$ = -0.175 in the uncracked state.

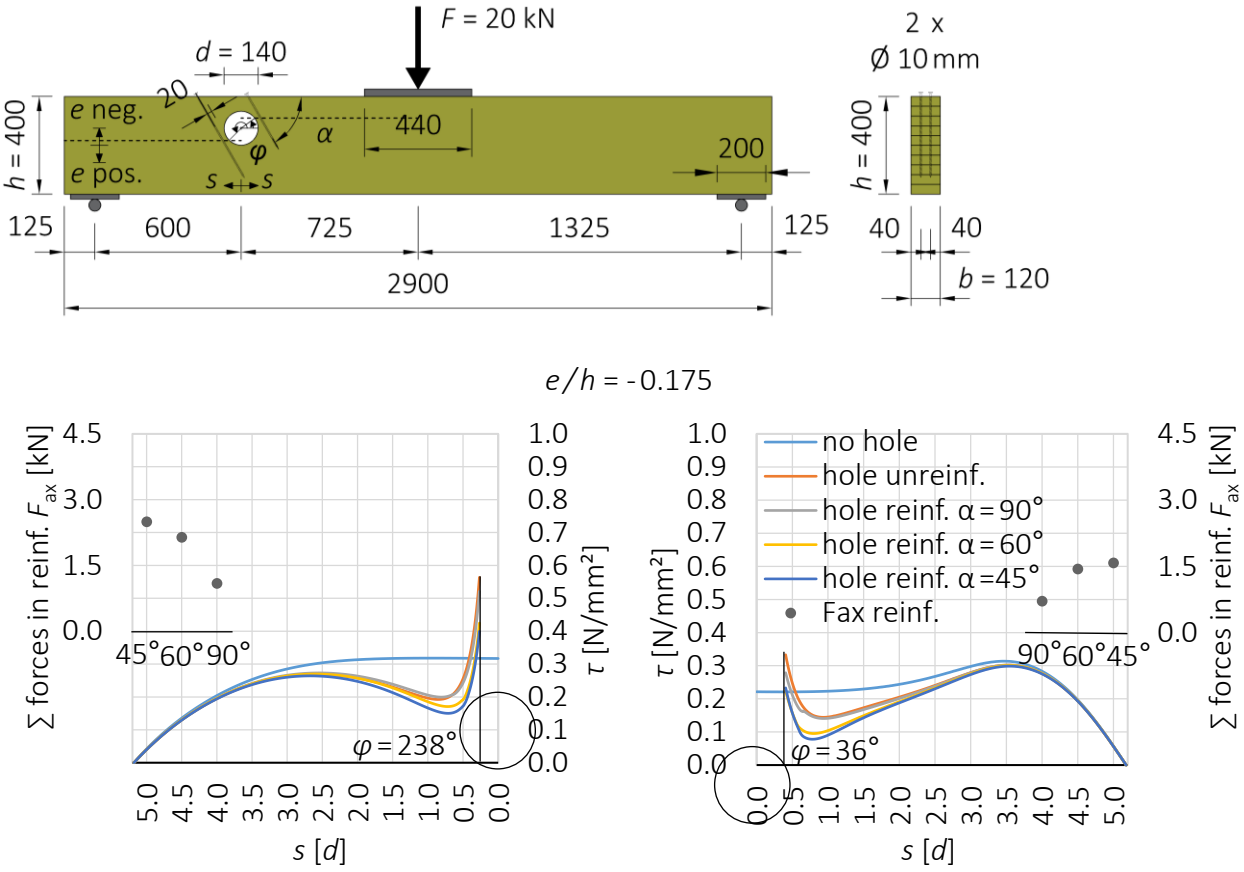


*Figure 11: Distributions of shear stresses along two paths representing planes of potential crack formations*

Regarding the reduction of shear stresses in dependence of the inclination of the reinforcing elements an inclination of $\alpha$ = 90° shows almost no effect due to the low stiffness perpendicular to the screw axis. Inclined applications result in a more pronounced reduction whereby the largest effect is obtained for an inclination of $\alpha$ = 45°.

# 4 Design approach

## 4.1 Individual holes arranged eccentrically

Basis of the following design approach is a parametric study within the context of numerical simulations (*b/h* = 120 mm/400 mm; *V* = 10 kN; *M* = 16 kNm). The results received therein were benchmarked against the experimental results. A comparison of test results and estimated load-bearing capacities based on Weibull theory showed good agreement (see Danzer et al. (2016) and Danzer et al. (2017) for more information), hence it was decided to transfer this approach into the existing design format of the German National Annex DIN EN 1995-1-1/NA (2013), see equations (1) to (9).

$$\frac{\frac{F_{t,90,V}}{l_{t,90,V}} + \frac{F_{t,90,M}}{l_{t,90,M}}}{0.5 \cdot b \cdot k_{vol} \cdot f_{t,90}} \leq 1.0 \tag{1}$$

with $$F_{t,90,V,I/III} = \frac{V \cdot 0.7 \cdot d}{4 \cdot h} \cdot \left[3 - \left(\frac{0.7 \cdot d}{h}\right)^2\right] \cdot k_{ecc} \tag{2}$$

$$k_{ecc} = 0.1 + \frac{d}{h} + 4.5 \cdot \frac{h_{ro/ru}}{h} + 0.2 \cdot \frac{d}{h} \cdot \frac{h_{ro/ru}}{h} - 4.9 \cdot \left(\frac{h_{ro/ru}}{h}\right)^2 \tag{3}$$

$$l_{t,90,V,I/III} = 1.3 \cdot d \tag{4}$$

and $$F_{t,90,M,I} = M \cdot \frac{d}{h^3} \cdot Max\begin{Bmatrix} -0.62 \cdot (e - 0.13 \cdot d) \\ -0.2 \cdot (e - 0.45 \cdot d) \\ 0.3 \cdot (e - 0.08 \cdot d) \end{Bmatrix} \tag{5}$$

$$l_{t,90,M,I} = 0.8 \cdot d \cdot \left(1 - \frac{e}{d}\right) \qquad with\ 0.6 \cdot d \leq l_{t,90,M,I} \leq 1.0 \cdot d \tag{6}$$

$$F_{t,90,M,III} = M \cdot \frac{d}{h^3} \cdot 0.22 \cdot (e + 0.19 \cdot d) \tag{7}$$

$$l_{t,90,M,III} = 0.4 \cdot d \tag{8}$$

$$k_{vol} = \left(\frac{V_0}{0.072 \cdot b \cdot d^2 \cdot \pi}\right)^{0.2} \qquad with\ V_0 = 0.01 m^3 \tag{9}$$

According to equation (1) the load cases shear force *V* and moment *M* are considered with individual distribution lengths $l_{t,90}$ in the form of a simplified addition regardless the differing locations of the individual maxima. In contrast to the existing design format two possible locations of maximum stresses (quadrant I and III) have to be taken into account for eccentric arrangements, see Figure 12. In case of the shear force *V* the established equation to determine the resultant force perpendicular to the grain of a hole located centrically was extended by a factor $k_{ecc}$ to account for the eccentricity of the hole, see equations (2) and (3). If quadrant I is considered, the distance to the upper edge $h_{ro}$ has to be used, in case of quadrant III the distance to the lower edge $h_{ru}$.

In case of the moment *M* the resultant forces in the two different quadrants were approximated by sectionally linear functions, see equations (5) and (7).

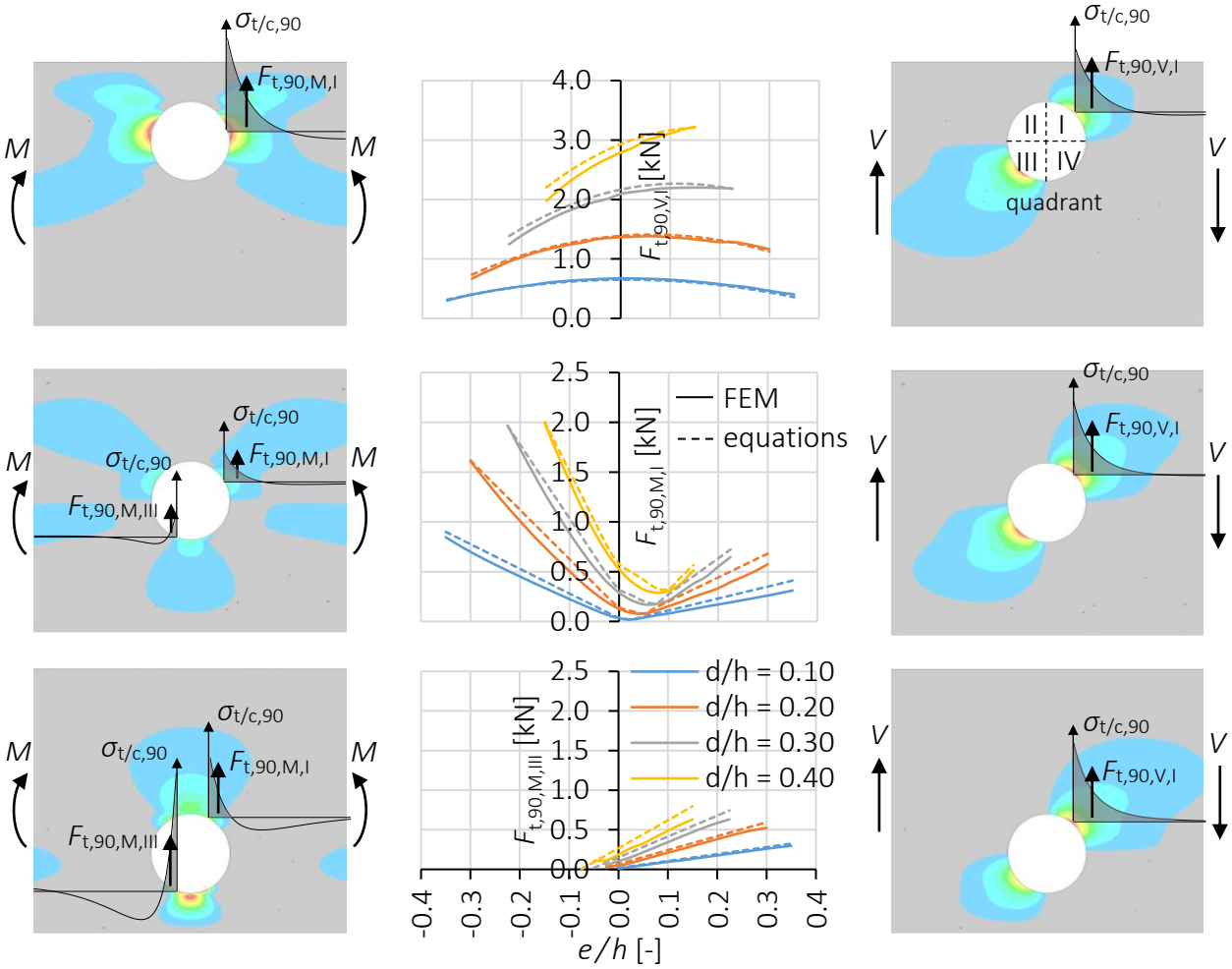


*Figure 12: Comparison of resultant forces perpendicular to grain (FEM vs. equations (2), (3), (5) and (7))*

In order to obtain the best possible agreement to experimental results the individual distribution lengths $l_{t,90}$ based on numerical investigations were slightly adapted, resulting in equations (4), (6) and (8). The volume defined by the expression in the denominator of equation (9) has the geometry of a segment of a ring with an aperture angle $\vartheta = 50°$, a radial extension of $\Delta r = 3/8 \cdot d$ and a thickness of the beam width $b$. A variation of these geometrical parameters had only a negligible effect on the results, hence the definition mentioned above is assessed sufficient and insensitive with respect to small changes of its parameters.

For assessment of the safety level a comparison of test results and the presented design approach at the level of characteristic values is shown in Figure 13. In addition to own test results of holes arranged eccentrically also test results of holes arranged centrically, based on investigations of Aicher & Höfflin (2006), were used. The characteristic values of the test series were determined based on a logarithmic normal distribution according to EN 14358 (2016) in combination with a global coefficient of variation

($COV_g$ = 15,8%) according to EN 14545 (2008), determined by considering all test results shown in Figure 13. The characteristic strength in tension perpendicular to the grain used in the design approach was $f_{t,90,k}$ = 0.5 N/mm².

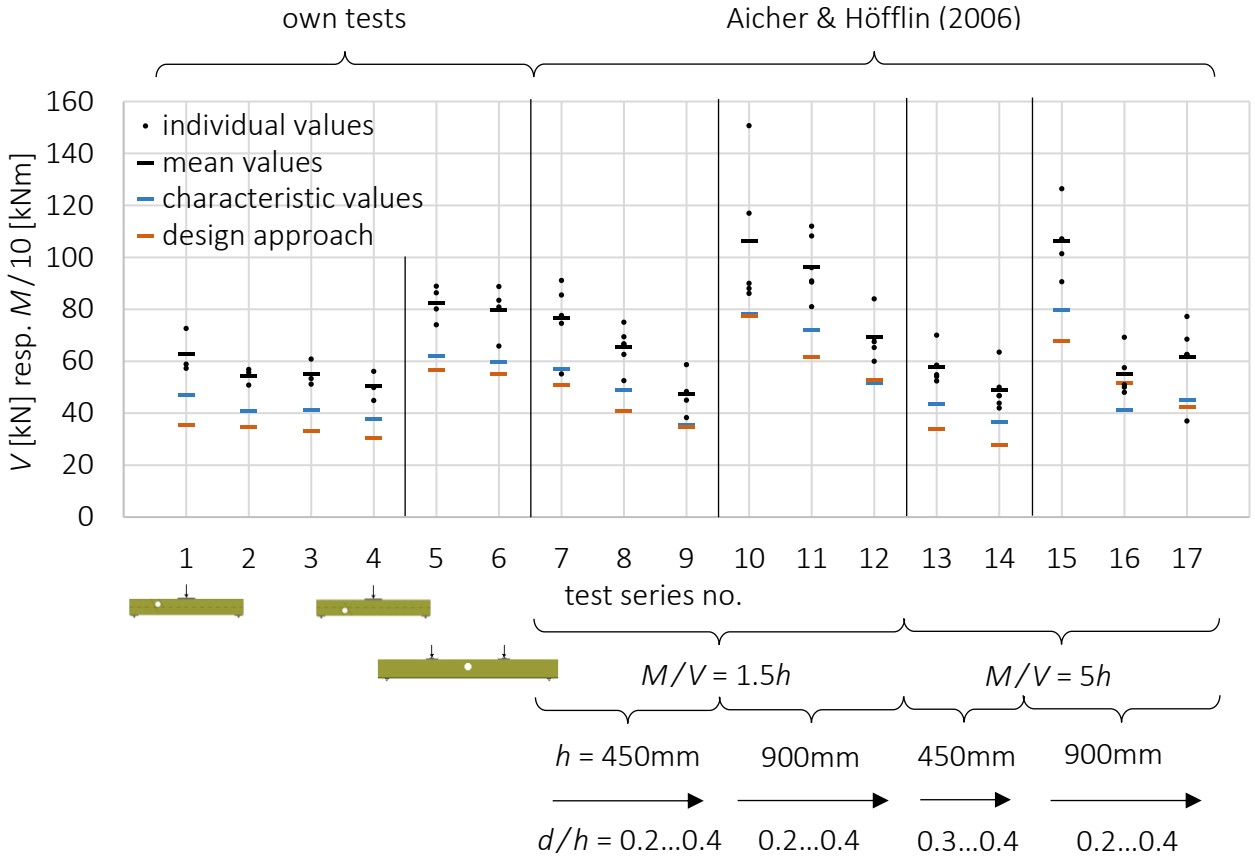


*Figure 13: Comparison of test results vs. design approach at the level of characteristic values (load level: full crack over the whole beam width)*

With the exception of test series no. 16 the design approach does not exceed the characteristic values of the experimental results. The results of test series no. 16 is assumed less relevant because of several reasons. Test series 15 – 17 show no clear trend although the diameter is increasing continuously whereas the other parameters remain constant. A comparison of test series 13 and 16 indicates a lower load-bearing capacity for the configuration featuring a beam height twice as large. A comparison of different ratios *M/V* (test series 10 – 12 with 15 – 17) shows only a marginal influence in cases of *d/h* = 0.20 and 0.40 but a pronounced one in case of *d/h* = 0.30.

## 4.2 Design of inclined reinforcement

With regard to designing inclined reinforcing elements, two different approaches were pursued to obtain the axial forces in the reinforcement. Towards this aim simplified numerical simulations of the partially cracked state in the form of a specified crack length *d*/2 were done.

The first approach is based on forces resulting from the stress distribution in tension perpendicular to the grain (uncracked state), which are converted by trigonometric functions in dependence of the angle of the inclined reinforcing elements, see Figure 14. A comparison of this procedure with axial forces in the reinforcing elements obtained with the numerical model mostly resulted in conservative results but also in non-conservative results.

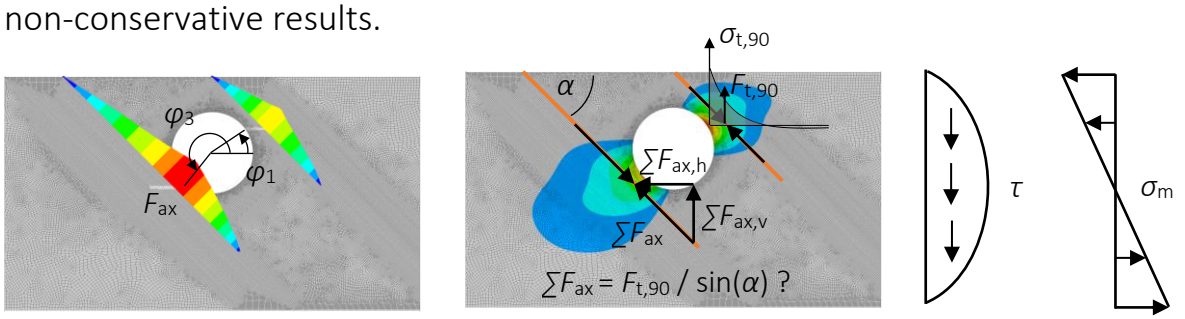


*Figure 14: Scheme showing the determination of the axial forces in the reinforcement based on resultant forces in tension perpendicular to the grain*

The second approach is based on shares of the horizontal shear flow due to a shear force *V* at the expected levels of crack formation, see Figure 15. Here, the fact that shear stresses at a hole also occur because of a moment *M,* is neglected for reason of simplification. Based on the horizontal components of the axial forces in the reinforcing elements obtained in the numerical model a length of about 0.3*d* was determined for an inclination $\alpha$ = 60° and a length of about 0.55*d* was determined for $\alpha$ = 45° (*d* hole diameter). Strain measurements inside the threaded rods realized during the large-scale tests confirm the order of magnitude but reveal slightly lower values compared to the simulations which were based on the small-scale tests reinforced by fully threaded screws.

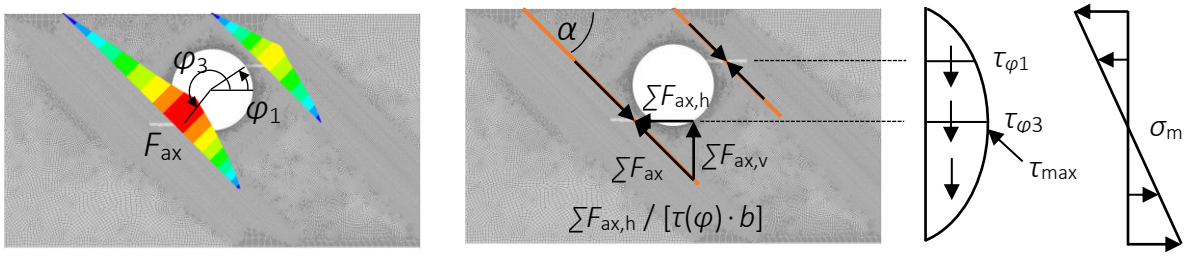


*Figure 15: Schematically figure of determining the axial forces of the reinforcement based on resultant shares of the horizontal shear flow*

Due to the simplified nature of the numerical considerations and the limited variation of parameters no general design concept can be given at this stage. Towards this aim, further investigations are necessary.

## 4.3 Groups of holes

### *4.3.1 Arrangement in horizontal direction*

With regard to groups of holes arranged in horizontal direction the mutual influence in dependence of the clear distance $l_z$ was also quantified in numerical parametric studies. Considering the unreinforced state, load-bearing capacities (determined using Weibull theory, see chapter 3.1) of groups of holes were compared to those of the respective individual holes. In this context load-bearing capacities describe a failure in tension perpendicular to the grain in the form of a crack over the whole beam width. In Figure 16 the general procedure as well as the varied parameters are shown.

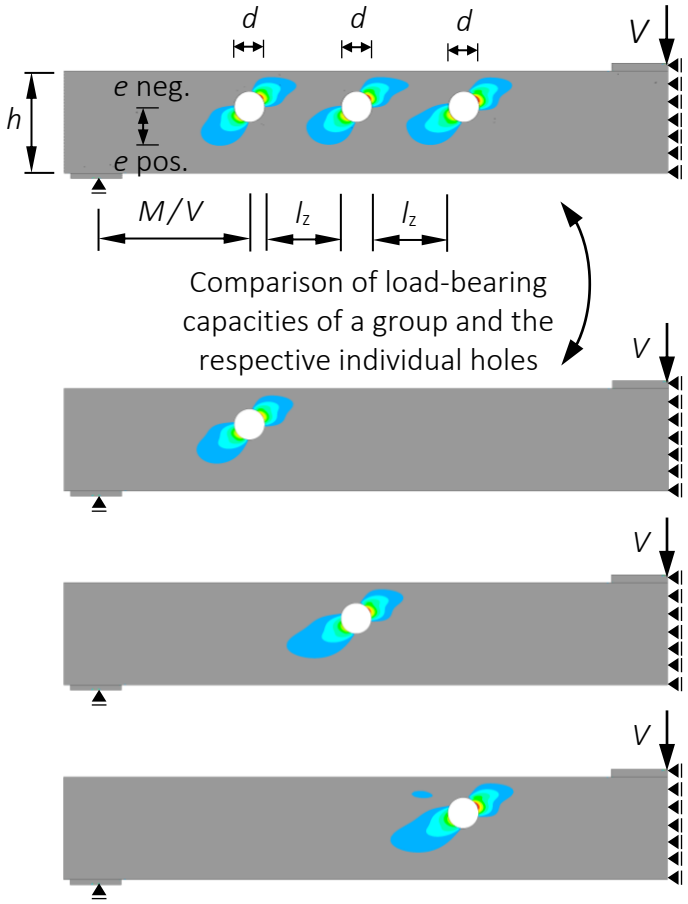


Parameters:

- number of holes:
  $n$ = 2; 3
- hole diameter:
  $d/h$ = 0.10; 0.30
- clear distance:
  $l_z = 2.0h - 0.125h/0.25h$
- eccentricity:
  $e/h$ = -0.15; 0.00; 0.15
- ratio $M/V$:
  $M/V = 1.5h$; $6.0h$; “∞“

*Figure 16: Procedure and varied parameters for determining the influence of the clear distance $l_z$*

The numerical parameter study shows that the mutual influence is not only dependent on the clear distance $l_z$ but also on the location in the beam, i.e. in general on the situation of loading. Thereby an increasing ratio $M/V$ has a positive effect, i.e. the most critical location is the region near the supports, dominated by shear forces. The mutual influence also is affected by the number of holes in the form of a slightly more pronounced influence in case of three holes.

Regardless the number of holes and the location in the beam the following reduction factor for the load-bearing capacity of a group was derived for the most critical situation ($n$ = 3; $M/V$ = 1.5$h$):

$$k_{space,hor} = Min\left\{\begin{array}{c} 1 \\ 1 - 0.2 \cdot \dfrac{1.5 \cdot h - l_z}{1.5 \cdot h} \\ 1 - 0.4 \cdot \dfrac{5 \cdot d - l_z}{5 \cdot d} \end{array}\right\} \qquad (10)$$

limitations:

- $n \leq 3$
- $d/h \leq 0.30$
- $l_z \geq 1d$

In Figure 17 this reduction factor is compared to the numerical results.

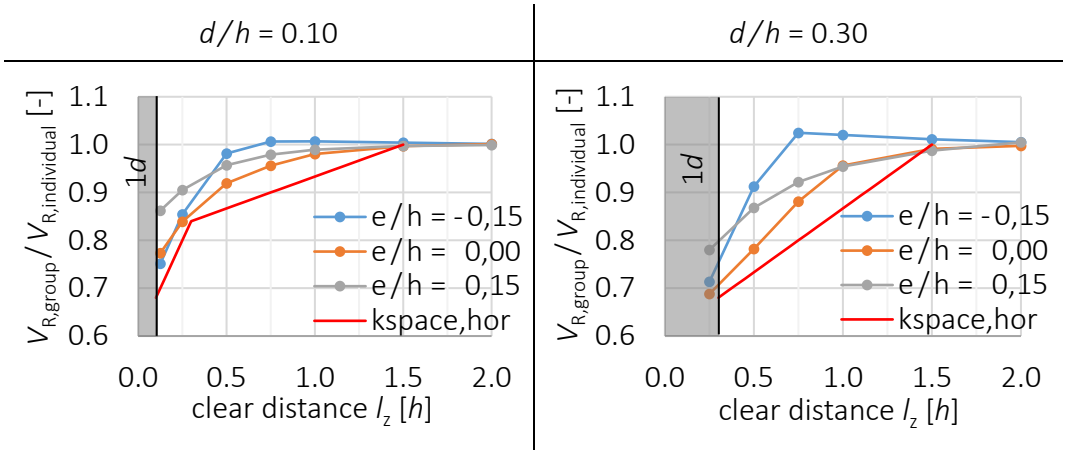


*Figure 17: Comparison between the derived reduction factor and results from simulations for horizontal groups of three holes (M/V = 1.5h)*

A comparison between equation (10) and the test results of the small-scale tests is debatable due to the violated limitations ($d/h$ = 0.35). However, an extrapolation of equation (10) would result in a conservative reduction compared to the test results.

### *4.3.2 Arrangement in vertical direction*

The structural behaviour of groups of holes arranged in vertical direction was investigated in a similar way to those arranged in horizontal direction. Due to geometrical limitations the hole diameter was limited to $d/h$ = 0.15. By means of these investigations the following reduction factor could be derived:

$$k_{space,vert} = Min\left\{\begin{array}{c} 1 \\ 1 - 0.15 \cdot \dfrac{5 \cdot d - l_z}{5 \cdot d} \end{array}\right\} \qquad (11)$$

limitations:

- $n \leq 3$
- $d/h \leq 0.15$
- $l_z \geq 1d$
- symmetric arrangement

In Figure 18 a comparison of this reduction factor and the numerical results is shown for the most critical case.

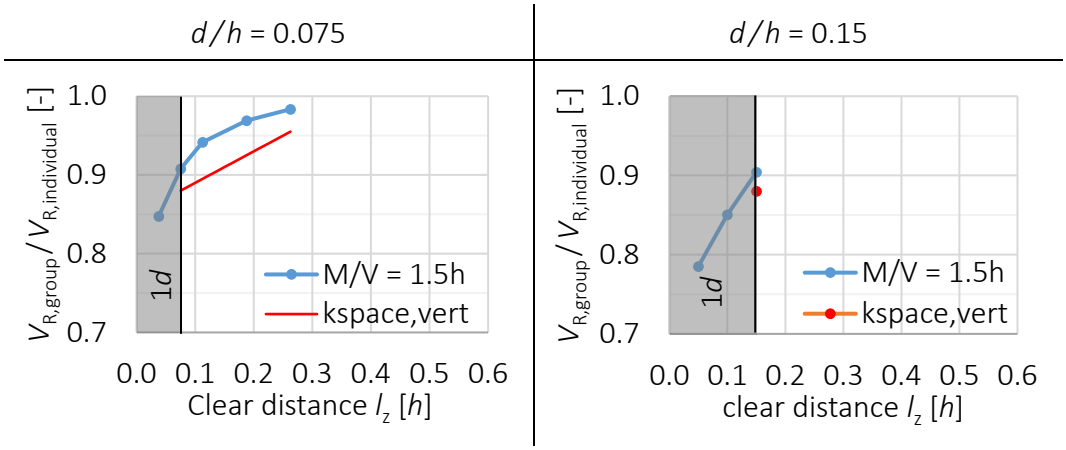


*Figure 18: Comparison between the derived reduction factor and results from simulations for vertical groups of three holes (M/V = 1.5h)*

A comparison between equation (11) and test results of the small-scale tests is also debatable due to the violated limitations. However, an extrapolation of equation (11) would be on the safe side compared to the test results.

# 5 References

Aicher, S., Höfflin, L. (2006): Tragfähigkeit und Bemessung von Brettschichtholzträgern mit runden Durchbrüchen – Sicherheitsrelevante Modifikationen der Bemessungsverfahren nach Eurocode 5 und DIN 1052. Forschungsbericht. MPA Stuttgart.

Danzer, M., Dietsch, P., Winter, S. (2016): Reinforcement of round holes in glulam beams arranged eccentrically or in groups. World Conference on Timber Engineering 2016, Conference Proceedings. Vienna, Austria.

Danzer, M., Dietsch, P., Winter, S. (2017): Einfluss exzentrisch positionierter Einzeldurchbrüche und Gruppen von Durchbrüchen auf die Tragfähigkeit von Brettschichtholzträgern – Entwicklung von Bemessungsverfahren und Konstruktionsregeln für Verstärkungsmaßnahmen. Schlussbericht zu IGF-Vorhaben 18048N. Lehrstuhl für Holzbau und Baukonstruktion, TU München.

EN 1995-1-1 (2004): Design of timber structures – Part 1-1: General – Common rules and rules for buildings. CEN. Brussels.

DIN EN 1995-1-1/NA (2013): National Annex – Nationally determined parameters – Eurocode 5: Design of timber structures – Part 1-1: General – Common rules and rules for buildings. DIN. Berlin.

EN 14358 (2016): Timber structures – Calculation and verification of characteristic values. CEN. Brussels.

EN 14545 (2008): Timber structures – Connectors – Requirements. CEN. Brussels.

Höfflin, L. (2005): Runde Durchbrüche in Brettschichtholzträgern – Experimentelle und theoretische Untersuchungen. Dissertation. Schriftenreihe Heft 90. MPA Universität Stuttgart.

# Discussion

The paper was presented by M Danzer

*S Aicher received clarification that in Figure 17 effect of multiple holes in horizontal direction the minimum clear distance used was 1d.*